Time resolved measurements of hydrogen ion energy distributions in a pulsed 2.45 GHz microwave plasma

A. Megía-Macías, O. D. Cortázar, O. Tarvainen, and H. Koivisto

Citation: Physics of Plasmas **24**, 113501 (2017);
View online: https://doi.org/10.1063/1.5001488
View Table of Contents: http://aip.scitation.org/toc/php/24/11
Published by the American Institute of Physics

Time resolved measurements of hydrogen ion energy distributions in a pulsed 2.45 GHz microwave plasma

A. Megía-Macías,[1,a)] O. D. Cortázar,[2] O. Tarvainen,[3] and H. Koivisto[3]
[1]*Department of Mechanics, Design and Industrial Management, Faculty of Engineering, University of Deusto, Bilbao, Spain*
[2]*University of Castilla-La Mancha, Ciudad Real, Spain*
[3]*Accelerator Laboratory, Department of Physics, University of Jyväskyla, Jyväskyla, Finland*

(Received 24 August 2017; accepted 12 October 2017; published online 27 October 2017)

A plasma diagnostic study of the Ion Energy Distribution Functions (IEDFs) of H^+, H_2^+, and H_3^+ ions in a 2.45 GHz hydrogen plasma reactor called TIPS is presented. The measurements are conducted by using a Plasma Ion Mass Spectrometer with an energy sector and a quadrupole detector from HIDEN Analytical Limited in order to select an ion species and to measure its energy distribution. The reactor is operated in the pulsed mode at 100 Hz with a duty cycle of 10% (1 ms pulse width). The IEDFs of H^+, H_2^+, and H_3^+ are obtained each 5 μs with 1 μs time resolution throughout the entire pulse. The temporal evolution of the plasma potential and ion temperature of H^+ is derived from the data. It is shown that the plasma potential is within the range of 15–20 V, while the ion temperature reaches values of 0.25–1 eV during the pulse and exhibits a fast transient peak when the microwave radiation is switched off. Finally, the ion temperatures are used to predict the transverse thermal emittance of a proton beam extracted from 2.45 GHz microwave discharges. *Published by AIP Publishing.* https://doi.org/10.1063/1.5001488

I. INTRODUCTION

The Ion Energy Distribution Functions (IEDFs) of the ion species involved in a hydrogen plasma are of interest for several reasons, e.g., to understand the ion dynamics within the discharge, compare the rates of certain plasma chemical reactions especially in discharges consisting of molecular species, and to predict the thermal properties of the extracted ion beams. Measurements of time resolved IEDFs have been reported for Argon microwave/RF plasmas applied to functional coatings such as optical protective barriers and hard films in order to determine the total energy delivered by impacting ions on a surface.[2] This diagnostic technique could give valuable information when used on a 2.45 GHz Electron Cyclotron Resonance (ECR) plasma typically applied for high-current light ion sources. In such devices, the role of electrons as responsible for the energy coupling between the plasma and RF or microwaves[3–5] is especially critical and well-studied. However, the dynamics of energy transfer processes between electrons and ions by the Coulomb interaction and especially by inelastic collisions, e.g., molecular dissociation and ionization, is less understood. The information on ion energy distribution can be used for predicting the contribution of the ion temperature on the transverse momentum spread (emittance) of the extracted ion beams and optimizing the source parameters for the production of different molecular species of, e.g., hydrogen ions, which has been the focus of recent studies.[6–10]

In this work, the temporal evolution of the H^+, H_2^+, and H_3^+ IEDFs is presented for the ignition and decay transients, as well as the steady-state of the discharge pulse. The IEDFs are used to determine the temperature of the ion population, which affects the beam quality, i.e., the transverse emittance, of the extracted ion beam[11] in 2.45 GHz microwave ion sources. The obtained ion temperatures are used for calculating the resulting thermal emittance. The results are compared to measured emittance values from different 2.45 GHz microwave ion sources to determine the relative importance of thermal and magnetic emittance components.

To the best of the authors' knowledge, this is the first time that the ion temperature is measured directly for H^+, H_2^+, and H_3^+ in a 2.45 GHz ECR plasma. Temperatures of most ion species can be derived from optical measurements with high-resolution spectrometers by observing the Doppler broadening of the emission lines of the ions. However, for H^+, this is impossible as the ion is fully stripped and thus has no electronic transitions available for spectroscopic purposes. This makes the results presented in this work of special relevance as 2.45 GHz plasma sources are very often used as H^+ ion sources.

II. EXPERIMENTAL SETUP

We have carried out our studies of the Ion Energy Distribution Functions (IEDFs) for the main ion species in a 2.45 GHz hydrogen plasma reactor called TIPS (Test-bench for Ion source Plasma Studies).[12] The reactor is operated in the pulsed mode at 100 Hz with a duty cycle of 10% (1 ms pulse width). The measurements are conducted by using a HIDEN Plasma Ion Mass Spectrometer Model EQP[1] that uses a 45° energy sector analyzer in tandem with a quadrupole mass analyzer. Such configuration is able to select a particular ion (mass and charge) to measure the corresponding energy distribution. The spectrometer is capable of running energy scans from 0 to 100 eV at 0.05 eV increments/

a)Electronic mail: ana.megia@deusto.es

0.25 eV FWHM. The IEDFs are obtained every 5 μs with 1 μs time resolution during the entire pulse duration and, to ensure an adequate signal to noise ratio, each temporal data point of the IEDF is taken over 10 consecutive pulses and averaged.

Figure 1 shows how the spectrometer is attached to the plasma reactor. Note that microwaves are injected into the plasma chamber (a) from the left side through a microwave coupling system[12] (b) and the ion spectrometer probe is connected to a diagnostics port (c) where a fiber optics feedthrough (e) is used to obtain a light signal from the plasma to monitor the pulse-to-pulse repeatability of the discharge properties. The ion spectrometer probe (d) is a stainless steel cylinder of 40 mm diameter with an incorporated extraction system to obtain a small sample of particles through a 50 μm pinhole. The pinhole nozzle of the spectrometer is aligned flush with the axial wall of the discharge chamber, often referred as the plasma electrode in ion sources, thus maintaining the dimensions and RF cavity properties of the original chamber. The ion spectrometer has a pumping system that maintains the gas in the discharge chamber at a pressure of 3.8×10^{-3} mbar, while the pressure in the instrument is between 10^{-7} and 10^{-8} mbar, which guarantees the collision-free transport of the ions and enables proper working conditions of the secondary electron multiplier (SEM). Both axial ends of the plasma chamber are covered by boron nitride discs (not visible in Fig. 1 for clarity reasons), which affects the species fraction of the hydrogen discharge.[13] Holes for pumping, pressure gauge, and gas inlet were made on the microwave injection side disc, and holes for optical diagnostics and ion extraction were made on the diagnostics side disc. A bidirectional microwave coupler inserted into the microwave waveguide provides the incoming and reflected power signals.

A precise synchronization is required to perform the time resolved measurements. The internal delay generator of the ion spectrometer is controlled with a TTL pulse from a pulse delay generator which is triggered by the positive slope of the incoming power signal. Figure 2 shows typical oscilloscope traces used for the synchronization.

A sequence of consecutive measurements every 5 μs with a time resolution of 1 μs was programmed into the acquisition system to obtain the evolution of H^+, H_2^+, and H_3^+ IEDFs during the entire length of the 1000 μs plasma pulse. The scan starts from the leading edge of the microwave pulse where no particle counts are recorded and goes up to 1200 μs, i.e., 200 μs after the trailing edge of the microwave pulse, where data corresponding to decaying plasma are still recorded.

Figure 3 shows the magnetic field profile used during the described experiment in a 2 D axial projection of the plasma chamber. The diagnostic port is on the right and the microwave injection on the left. The given magnetic field profile is typical to 2.45 GHz microwave ion sources with the resonance zone adjacent to the microwave window and $B > B_{ECR}$ in the majority of the plasma volume.[14] The dimensions of the plasma chamber are 85 mm in diameter (vertical) by 113 mm in length (horizontal). The incident microwave power was 1500 W. The simulation of the magnetic field was performed using FEMM software.[15]

III. RESULTS

Figure 4 shows the results obtained under the experimental conditions described above. Note that for clarity, only IEDFs obtained at every 50 μs have been plotted.

All IEDFs shown in the figure exhibit a Gaussian distribution peaking at approximately 15–20 eV. The apparent shift of the distributions is presumably caused by the (positive) plasma potential. Such positive potential across the plasma sheath provides the ions entering the analyzer with a longitudinal velocity that is reflected on the IEDFs as a positive shift and must then be taken into account.

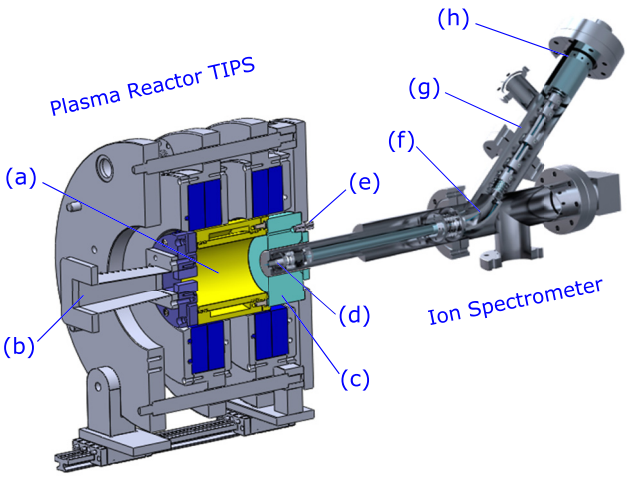

FIG. 1. Experimental setup: (a) plasma chamber, (b) microwave coupling system, (c) diagnostics port, (d) ion spectrometer probe, (e) fiber optics port, (f) 45° energy sector analyzer, (g) quadrupole mass analyzer, and (h) ion detector.

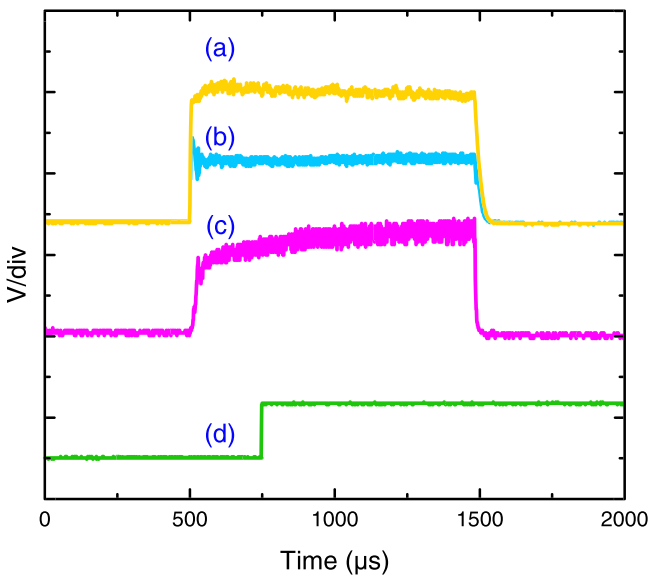

FIG. 2. Typical oscilloscope traces used for data acquisition synchronization: incoming microwave power signal (a), reflected microwave power signal (b), integrated visible light emission signal from the plasma (c), and monitoring pulse from the ion spectrometer controller with the leading edge, indicating the time instant at which the IEDFs are measured (d).

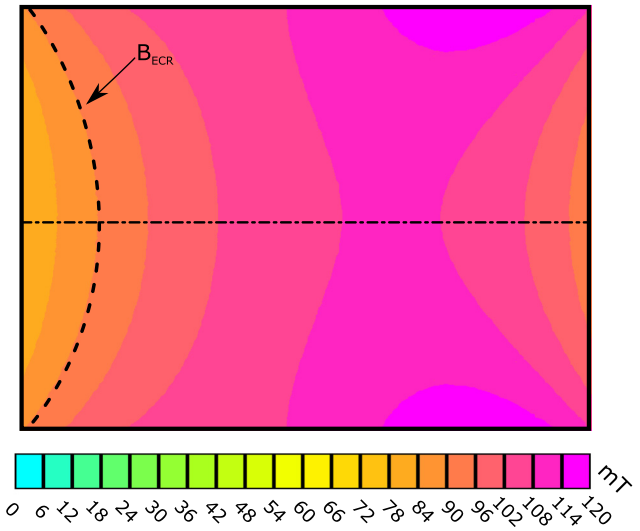

FIG. 3. A 2D projection of the magnetic field distribution inside the plasma chamber. The axis of the cylindrical chamber is marked with a dashed line. The microwave injection is on the left side, while the diagnostic port is on the right side.

Considering that our magnetic profile does not produce a magnetic mirror (that would filter the ion escape velocities) and the (nearly) Gaussian shape of the shifted distribution, we can assume that the transverse velocities of the ions follow a Maxwell-Boltzmann *velocity* distribution:

$$f(\bar{v}) = \left(\frac{m}{2\pi k T_i}\right)^{\frac{3}{2}} \exp\left(\frac{-m\bar{v}^2}{2kT_i}\right), \tag{1}$$

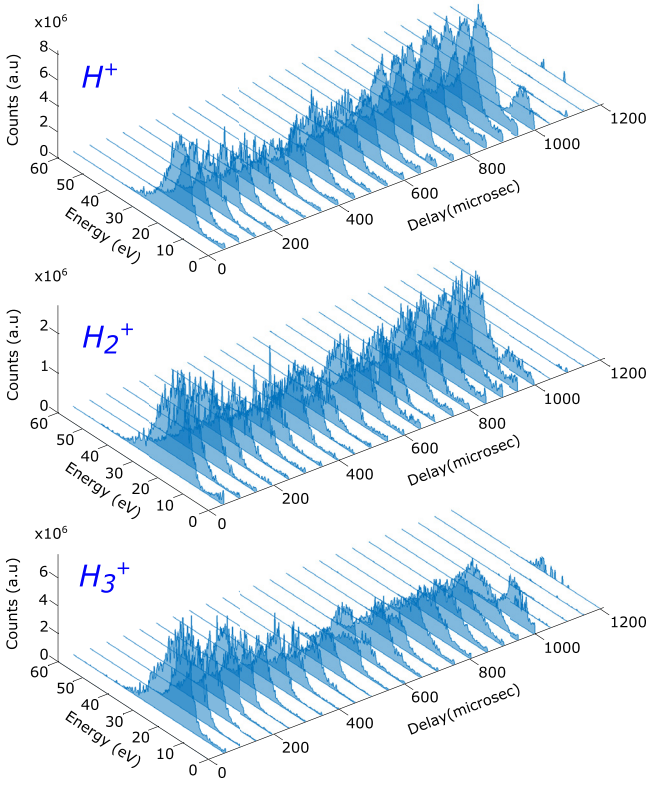

FIG. 4. IEDFs for H^+, H_2^+, and H_3^+ obtained with a time resolution of 1 μs every 50 μs during the entire microwave pulse.

where kT_i is the ion temperature, m is the ion mass, and $\bar{v}$ is the (transverse) ion velocity. Considering the plasma to be in local equilibrium during the measurement of each curve, the peak of the velocity distribution should be at zero because the particles within the plasma do not have a global direction of motion. However, the afore-mentioned energy shift due to the plasma potential causes the particles entering the analyzer to have a longitudinal drift velocity towards the detector. Thus, the velocity distribution of the recorded ions can be described by a drifting Maxwellian distribution, i.e.,

$$f(\bar{v}) = \left(\frac{m}{2\pi k T_i}\right)^{\frac{3}{2}} \exp\left(\frac{-m(v - v_{shift})^2}{2kT_i}\right), \tag{2}$$

where the (longitudinal) drift velocity v_{shift} is related to the plasma potential V_p as

$$v_{shift} = \sqrt{\frac{2qV_p}{m}}, \tag{3}$$

where q is the ion charge, namely, the elementary charge for singly charged ions.

The recorded IEDFs can be converted into velocity distributions (IVDFs) and fitted with a drifting Maxwellian distribution to obtain the plasma potential V_p and ion temperature kT_i. As an example, Fig. 5 shows in detail one of the measured IEDFs converted to a normalized IVDF. In particular, it corresponds to H_3^+ recorded at 500 μs delay. The blue line corresponds to the least mean square fit of a normalized drifting Maxwell-Boltzmann distribution. The corresponding plasma potential and ion temperature are 17.3 V and 0.3 eV, respectively.

Similar fitting was performed for all consecutive IVDFs (241 in total) acquired for each ion species to obtain the temporal evolution of the ion temperature and the plasma potential along the plasma pulse. Figure 6 shows the evolution of the plasma potential and the ion temperature of H^+ ions during the plasma pulse. It is interesting to notice the peaks that

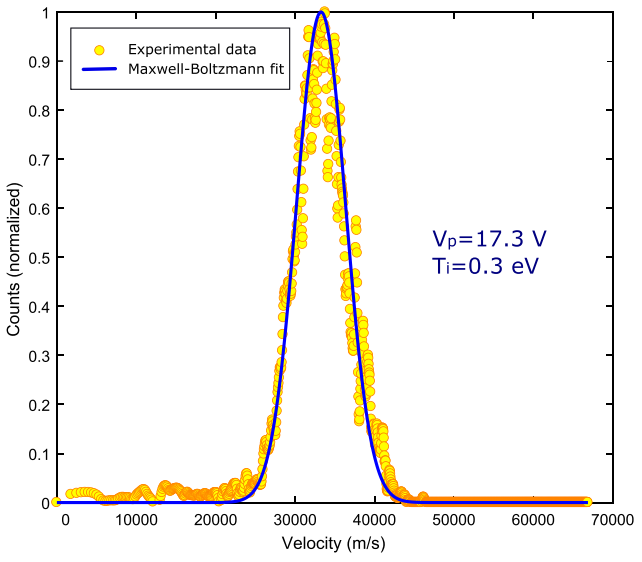

FIG. 5. Least mean square fitting of the experimental data to a normalized drifting Maxwell-Boltzmann velocity distribution.

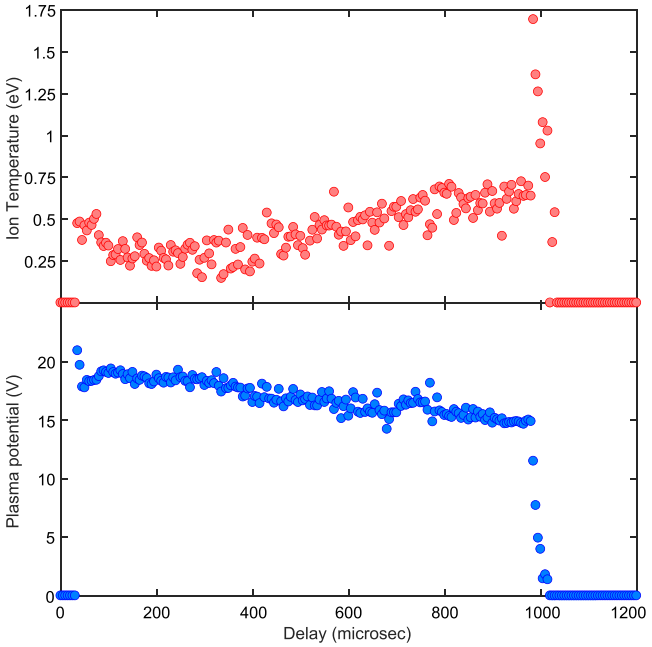

FIG. 6. Temporal evolution of the plasma potential and ion temperature obtained from IEDFs of H^+ ions.

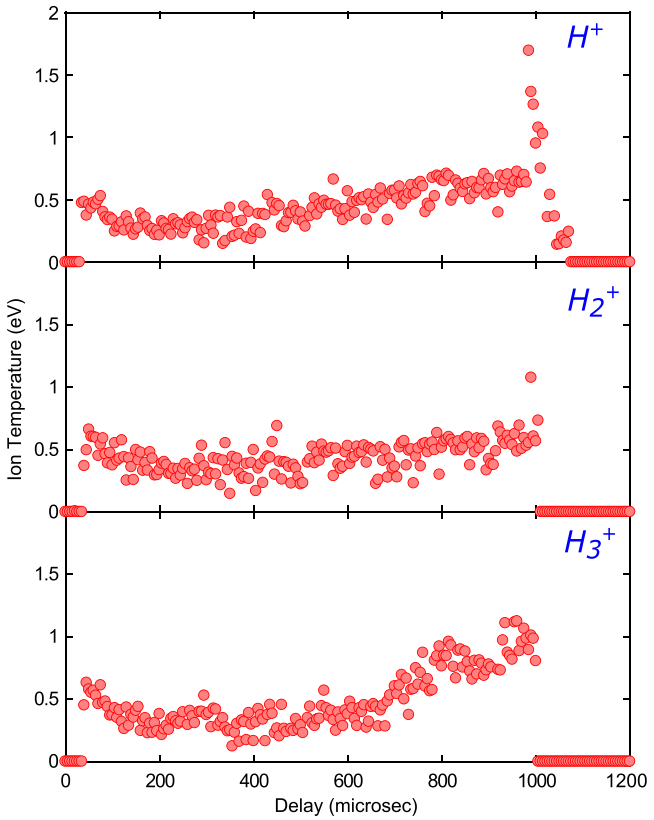

FIG. 7. Temporal evolution of the ion temperature for H^+, H_2^+, and H_3^+ ions.

can be observed in the ion temperature during the breakdown and decay. The ion temperature reaches 0.5 eV during the breakdown where the steady-state species fraction has not been reached as described in Ref. 16, then decays to 0.2–0.4 eV in approximately 150 μs, and afterwards, follows a monotonic increase to reach a value of 0.7 eV. Finally, a sharp peak reaching 1.75 eV in coincidence with the trailing edge of the microwave pulse is observed. The evolution of the plasma potential also presents a peak reaching 21 V during the breakdown and decreasing later to 17 V by the end of the pulse.

The values of T_i and V_p were also calculated from H_2^+ and H_3^+. As expected, the plasma potential values obtained from H^+, H_2^+, and H_3^+ IEDFs were within an error margin of 10% due to noise in the IEDF signals. The ion temperatures of different hydrogen ion species are presented in Fig. 7. The ion temperatures of all three species measured during the microwave pulse are <1 eV, which is often assumed to be the ion temperature in 2.45 GHz microwave discharges.

IV. DISCUSSION

2.45 GHz ECR discharges similar to TIPS are widely used as high-current light ion sources, in particular, for proton beam production.[17–21] In such application, the properties of the plasma have a strong effect on the quality of the extracted ion beam, which is typically characterized by the transverse emittance (ϵ) of the beam, which must be matched with the acceptance of the subsequent accelerator in (x,x'), (y,y') phase space. The quality of an ion beam is defined in terms of current and emittance. The emittance is affected by the ion temperature (thermal emittance), the rotation induced by the decreasing axial magnetic field of the ion source (magnetic emittance), and non-linear effects in the beam transport line (emittance growth). The minimum value of the normalized 1–*rms* transverse emittance of the extracted beam in the units of mm mrad can be calculated using the following expression:[22]

$$\epsilon_{rms,n} = 0.0164r\sqrt{\frac{kT_i}{M}} + 0.0402r^2\frac{BQ}{M}, \tag{4}$$

where r is the extraction aperture radius in mm, kT_i is the ion temperature in eV, M is the ion mass in amu, B is the magnetic field at the extraction aperture in units of Tesla, and Q is the ion charge state. The equation takes into account the thermal emittance (ion temperature) and the magnetic emittance (field strength at the extraction). In our case, the value of the magnetic field at the extraction is 96 mT for the experimental conditions discussed above.

Figure 8 shows a calculation of the evolution of the beam emittance during the plasma pulse for two different extraction apertures, namely, 3 and 5 mm, which correspond to the range of extraction aperture radii in proton ion sources. Figure 8(a) corresponds to an extraction aperture radius of 3 mm, while Fig. 8(b) corresponds to a radius of 5 mm. The blue dashed line represents the magnetic component of the emittance, while the green circles show the total emittance. The calculated emittance values are in relatively good agreement with experimental measurements reported in the literature for different ion sources such as TRIPS[17] (r= 3 mm, $\epsilon_{rms,n}$ = 0.07–0.28 π mm mrad, and I = 32–51 mA) or SILHI[18] (r = 4 mm, $\epsilon_{rms,n}$ = 0.33 π mm mrad, and I = 66 mA). Note that in the given references, π has been added to the unit of emittance to merely emphasize that the quoted value is the product of the phase space emittance ellipse half axes, not the area, i.e., the emittance values can be compared directly to those reported here.

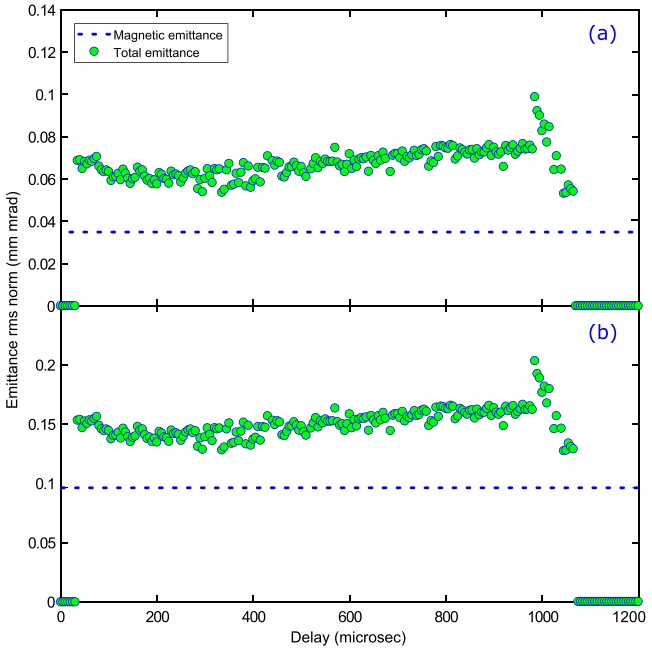

FIG. 8. H^+ emittance calculated from the measured ion temperatures and applied magnetic field. Extraction aperture radius r: 3 mm (a) and 5 mm (b).

The implication of Fig. 8 is that the contribution of the thermal and magnetic effects on the total emittance is approximately equal. Minimizing the emittance could therefore be accomplished by either reducing the ion temperature, which is considered challenging, or by tailoring the magnetic field profile to minimize the magnetic emittance. The latter could be accomplished by replacing the solenoid field by a permanent magnet cusp-field, fulfilling the resonance condition but resulting in zero field on the source axis.

ACKNOWLEDGMENTS

This project was conducted with the support of Grant Nos. UNCM13-1E-1551 and FIS2016-77132-R from the Ministry of Economy and Competitiveness of Spain.

This project received funding from the European Union's Horizon 2020 research and innovation programme under Grant Agreement No. 654002.

[1]HIDEN Analytical Ltd., see http://www.hidenanalytical.com/ for more details on the Plasma Ion Mass Spectrometer.
[2]A. Zabeida, A. Hallil, M. Wertheimer, and L. Martinu, J. Appl. Phys. **88**, 635 (2000).
[3]L. Celona, S. Gammino, G. Ciavola, F. Maimone, and D. Mascali, Rev. Sci. Instrum. **81**, 02A333 (2010).
[4]O. Tarvainen, T. Ropponen, T. Thuillier, J. Noland, V. Toivanen, T. Kalvas, and H. Koivisto, Rev. Sci. Instrum. **81**, 02A303 (2010).
[5]J. Jauberteau, I. Jauberteau, O. Cortázar, and A. Megía-Macías, Phys. Plasmas **23**, 033513 (2016).
[6]R. Xu, J. Zhao, S. Peng, Z. Yuan, Z. Song, J. Yu, and Z. Guo, Rev. Sci. Instrum. **79**, 02B713 (2008).
[7]Y. Xu, S. Peng, H. Ren, J. Zhao, J. Chen, T. Zhang, A. Zhang, Z. Guo, and J. Chen, Rev. Sci. Instrum. **85**, 02A943 (2014).
[8]O. Cortázar, A. Megía-Macías, O. Tarvainen, T. Kalvas, and H. Koivisto, Rev. Sci. Instrum. **87**, 02A704 (2016).
[9]O. Cortázar, A. Megía-Macías, O. Tarvainen, A. Vizcaíno-de Julián, and H. Koivisto, Plasma Sources Sci. Technol. **23**, 065028 (2014).
[10]O. Cortazar and A. Megia-Macias, IEEE Trans. Plasma Sci. **44**, 734 (2016).
[11]G. Brown, *The Physics and Technology of Ion Sources*, 2nd ed. (WILEY-VCH, 2004).
[12]A. Megía-Macías, O. D. Cortázar, and A. Vizcaíno-de Julián, Rev. Sci. Instrum. **85**, 033310 (2014).
[13]O. Waldmann and B. Ludewigt, Rev. Sci. Instrum. **82**, 113505 (2011).
[14]S. Gammino, L. Celona, G. Ciavola, F. Maimone, and D. Mascali, Rev. Sci. Instrum. **81**, 02B313 (2010).
[15]D. Meeker, see www.femm.info for Finite element method magnetics v4.2, 2010.
[16]O. Cortázar, A. Megía-Macías, O. Tarvainen, T. Kalvas, and H. Koivisto, Rev. Sci. Instrum. **86**, 083309 (2015).
[17]L. Celona, G. Ciavola, S. Gammino, F. Chines, M. Presti, L. Andò, and X. H. Gou, Rev. Sci. Instrum. **75**, 1423 (2004).
[18]P.-Y. Beauvais, R. Ferdinand, R. Gobin, J. M. Lagniel, P.-A. Leroy, L. Celona, G. Ciavola, S. Gammino, B. Pottin, and J. Sherman, Rev. Sci. Instrum. **71**, 1413 (2000).
[19]A. Efremov, V. Brkhterev, S. Bogomolov, G. Gulbekyan, A. N. Lebedev, V. N. Loginov, Y. I. Smirnov, and M. Leporis, Nucl. Instrum. Methods Phys. Res. B **204**, 368 (2003).
[20]S. Fiedler and H. P. Winter, Rev. Sci. Instrum. **63**, 2532 (1992).
[21]D. C. Wutte, M. A. Leitner, M. D. Williams, K. N. Leung, R. A. Gough, K. Saadatmand, and V. Benveniste, Rev. Sci. Instrum. **69**, 712 (1998).
[22]V. Toivanen, H. Kalvas, J. Koivisto, and T. O. Komppula, J. Instrum. **8**, P05003 (2013).